



A New Insight Into *Amicula*, a Genus of Tiny Marine Benthic Diatoms With the Description of Two New Tropical Species and the Largest Mitogenome Known for a Stramenopile

Romain Gastineau^{1*}, Chunlian Li², Matt P. Ashworth³, Andrzej Witkowski¹, Monique Turmel⁴, Ewa Górecka¹, Thomas A. Frankovich⁵, Anna Wachnicka⁶, Christopher S. Lobban⁷, Edward C. Theriot⁸, Christian Otis⁴, Przemysław Dąbek¹, Anna Binczewska¹ and Claude Lemieux^{4*}

OPEN ACCESS

Edited by:

Haifeng Gu,
Third Institute of
Oceanography, China

Reviewed by:

Yuhang Li,
Institute of Oceanology,
Chinese Academy of Sciences
(CAS), China
Yan Liu,
Harbin Normal University,
China

*Correspondence:

Romain Gastineau
romain.gastineau@usz.edu.pl
Claude Lemieux
claude.lemieux@bcm.ulaval.ca

Specialty section:

This article was submitted to
Marine Biology,
a section of the journal
Frontiers in Marine Science

Received: 11 May 2022

Accepted: 10 June 2022

Published: 20 July 2022

Citation:

Gastineau R, Li C, Ashworth MP, Witkowski A, Turmel M, Górecka E, Frankovich TA, Wachnicka A, Lobban CS, Theriot EC, Otis C, Dąbek P, Binczewska A and Lemieux C (2022) A New Insight Into *Amicula*, a Genus of Tiny Marine Benthic Diatoms With the Description of Two New Tropical Species and the Largest Mitogenome Known for a Stramenopile. *Front. Mar. Sci.* 9:941506. doi: 10.3389/fmars.2022.941506

¹Institute of Marine and Environmental Sciences, University of Szczecin, Szczecin, Poland, ²Institute of Ecological Sciences, South China Normal University, Guangzhou, China, ³Department of Molecular Biosciences, The University of Texas at Austin, Austin, TX, United States, ⁴Département de biochimie, de microbiologie et de bio-Informatique, Institut de Biologie Intégrative et des Systèmes, Université Laval, Québec, QC, Canada, ⁵Institute of Environment, Florida International University, Miami, FL, United States, ⁶South Florida Water Management District, West Palm Beach, FL, United States, ⁷Division of Natural Sciences, University of Guam, Mangilao, GU, United States, ⁸Section of Integrative Biology, The University of Texas at Austin, Austin, TX, United States

The current article focuses on the morphological and molecular characterization of the often inconspicuous genus *Amicula*. This recently erected genus from brackish and marine sediments was monotypic but here we describe two new tropical species: *Amicula micronesica* sp. nov. and *Amicula vermiculata* sp. nov. Once considered an incertae sedis genus regarding its higher rank taxonomy, its position among the family Diploneidaceae is proposed here by molecular phylogenetics. The complete plastid and mitochondrial genomes of *Amicula micronesica* sp. nov. are also presented here. It appears that the 177614-bp long mitogenome is the biggest yet recorded among stramenopiles, due to its invasion by 57 introns. Moreover, it utilizes the genetic code 4 for translation instead of the code 1 usually found among diatoms.

Keywords: diatom, *Amicula*, introns, mitogenome, plastome, benthic

INTRODUCTION

Diatoms (Bacillariophyta), one of the largest groups of photosynthetic microeukaryotes, are characterized by a multi-part exoskeleton built of glass-like opaline biosilica (Round et al., 1990). With a global distribution across oceans, marine planktonic diatoms are considered the major primary producer on a global scale (Field et al., 1998, Smol and Stoermer 2010). They play key roles in the sustainability of the littoral ecosystems (cf. Cox et al., 2020) including suspension feeders, thanks to their prominent place in the food web as primary producers (Houki et al., 2018).

The genus *Amicula* Witkowski et al., 2000 is a rarely-reported genus of tiny (<10 μm) marine diatoms, erected to accommodate a single species formerly described as *Navicula specululum* Witkowski (Witkowski 1994, Witkowski et al., 2000). The genus is characterized by its very small size, the short raphe branches terminating below the apices, a distinct central nodule and the

circumvalvar ring of areolae restricted to the valve margin. The transapical striae in *Amicula* are formed by large elliptical single areolae, occluded externally by cribra and internally by hymenate occlusions. Despite the very small size of the cells, light microscopy is usually sufficient to identify this genus but it is not possible to distinguish between different species without electron microscopy. Although described and documented from the central and western Baltic Sea as *Navicula nolens* (Simonsen 1959) and *Navicula speculum* (Witkowski 1994), the species was also illustrated, yet with an erroneous species name (i.e., *Navicula amphipleuroides*, Navarro, 1982) on mangrove prop roots in the Indian River Lagoon, Florida USA. The original description of *Amicula speculum* suggested a wide distribution, with the aforementioned Baltic Sea and Florida, evidenced also by records from Kenya (Witkowski et al., 2000; Witkowski, unpublished material). Since the description of the genus, no new species of *Amicula* have been described, but *Amicula speculum* was illustrated (though misidentified as *Diploneis* sp.) in Schmidt et al. (2018) from the Eastern Mediterranean and an unknown *Amicula* species with different areolar occlusions was identified as *A. speculum* (Nevrova and Petrov, 2019) from the Black Sea.

In the current article, we describe two new species, *Amicula micronesica* sp. nov. and *Amicula vermiculata* sp. nov., from the islands of Guam and near the Marquesas Keys in the Florida Keys archipelago USA, respectively. Their description is based on light and electron microscopy obtained on both wild samples and monoclonal cultures. Witkowski et al. (2000) did not attribute a position for *Amicula* in the broader classification of raphid diatoms when establishing the genus, as they could not find any characters shared between this genus and other raphid genera. Cox (2015), however, included *Amicula* among the Suborder of Naviculineae Hendey. Here, we introduced for the first time the use of molecular phylogenetics to assess the position of this genus. Additionally, we sequenced the mitochondrial and plastid genomes of *A. micronesica*. The mitogenome appears to be extremely complex and invaded by introns, representing the largest mitogenome ever obtained from a stramenopile.

MATERIAL AND METHODS

Isolation and Cultivation

Amicula micronesica was isolated from the sample collected on May 10, 2015, in Apra Harbor, Guam, USA (13° 27' 12" N, 144° 39' 12.56" E) and has previously received the isolate name GU52X-4 cfCalB7, with the voucher number HK478 in Edward C. Theriot's lab at the University of Texas at Austin, Texas, USA. *Amicula vermiculata* was isolated from a sample collected using a Ponar grab sampler in 20 m water depth on February 15, 2013, near the Marquesas Keys in Florida Keys archipelago, Florida, USA (24° 40' 53" N, 82° 19' 51" W) and has been registered as SZCZCH282 in the Szczecin Culture Collection, Szczecin, Poland. Both strains were isolated with micropipettes and cultivated in 250 mL Erlenmeyer flasks with F/2 medium (Guillard, 1975). The SZCZCH282 strain was cultivated under a

photoperiod of 14/10 h day/night, and an illumination of ca. 80 $\mu\text{mol photons m}^{-2} \text{ s}^{-1}$. Strain GU52X-4 cfCalB7 was maintained at 25°C in a Percival model I-36LL growth chamber under a 12/12 h day/night regimen.

Microscopy

The *A. vermiculata* strain SZCZCH282 was cultivated and prepared for examination at the University of Szczecin. The wild material from Florida and the monoclonal culture of SZCZCH282 were digested in 10% HCl to remove calcium carbonate and mineralize organic matter. After being washed several times with deionized water, they were boiled in 37% H_2O_2 . The washing process with deionized water was again repeated several times. For light microscope (LM) observations, the suspension was pipetted onto cover slips, left at room temperature for 24 hours until evaporation and mounted onto glass slides using Naphrax[®]. Frustules were imaged with a Zeiss Axio Imager A2 microscope equipped with a 100 × Plan Apochromatic objective with differential interference contrast (DIC) for oil immersion (NA 1.46). The images were captured with a Zeiss AxioCam ICc5 camera. For scanning electron microscopy (SEM) observations, specimens were collected onto a polycarbonate membrane filter with a 3- μm mesh size, attached to aluminum stubs and sputter-coated with 20 nm of gold using a Turbo-Pumped Sputter Coater Quorum Q 150OT ES. For transmission electron microscopy (TEM), a drop of cleaned suspension was placed onto a copper grid and left to dry at room temperature. Specimens were examined using a Hitachi SU 8010 microscope at the Podkarpackie Innovative Research Center of the Environment (PIRCE) at the University of Rzeszów. Observations were done with a HITACHI S-5500 microscope operated in STEM mode, which allows the same specimen to be observed in TEM and SEM modes in parallel. The Florida specimens were also observed and imaged using a JEOL-IT500HR field-emission scanning electron microscope operated at 5 kV and at a working distance of 9.4 mm.

For the strain HK478 of *A. micronesica*, the work was undertaken at the University of Texas at Austin. An aliquot of the culture was cleaned for microscopy using a 1:1:1 mix of culture, 37% H_2O_2 and concentrated nitric acid. This material was then washed with distilled water until the pH was neutral. Permanent mounts for LM were made by drying material onto glass coverslips and mounting to slides with Naphrax[®] mounting medium. For SEM preparation, cleaned culture material was dried onto 12 mm round coverslips and mounted onto aluminum stubs. Stubs were then coated with iridium using a Cressington 208 Bench Top Sputter Coater and observed with a Zeiss SUPRA 40 VP scanning electron microscope.

Sanger Sequencing of PCR Products

DNA was extracted from an exponentially growing culture of *A. vermiculata* using the Genomic DNA NucleoSpin[®] Plant II Kit (Qiagen, Germany) according to the manufacturer's instructions. This DNA preparation served as template for PCR amplification of the chloroplast *rbcL* gene, which was the only

one obtained by this protocol in the course of the study. The PCR reaction (25 μ L) contained 20 ng purified DNA template; 2.5 μ L 10x Dream Taq buffer (including 20 mM $MgCl_2$), 1 μ L Ultrapure dNTPs Set (5 mM each dATP, dCTP, dGTP, dTTP), 0.5 μ L of each primer at a concentration of 10 μ M and 0.15 μ L Dream Taq DNA polymerase (5 U/ μ L). The primers for PCR amplification were taken from Alverson et al. (2007). Conditions for PCR amplification were as follows: 94°C for 2 min, 35 cycles of (94°C for 15 s, 55°C for 15 s, 53°C for 1.15 min), and final extension at 72°C for 7 min. The PCR product was visualized in 1% agarose (Maximus, Poland) gel, purified using the Exo-BAP kit (EURx, Gdańsk, Poland) and sent to the oligo.pl DNA Sequencing Laboratory IBB PAS (Warsaw, Poland) for Sanger sequencing with the BigDye Terminator v. 3.1 chemistry and ABI3730 xl sequencer.

Next Generation Sequencing

Total DNA was extracted from *A. micronesica* according to Doyle and Doyle (1990) and was then sent to the Beijing Genomics Institute for sequencing on the DNBSEQ platform. In total, about 40 M of clean 150 bp paired-end reads were obtained. Assembly of the filtered reads was performed using SPAdes 3.14.0 (Bankevich et al., 2012), with a k-mer of 125. Contigs corresponding to the plastid genome (plastome) were recovered from the assembly by a blastn command-line query using the plastomes of pennate species from the genus *Haslea* as reference. The contigs corresponding to the mitogenome were found by performing a blastx command line query using a database of mitochondrial protein sequences from raphid pennate diatoms. When needed, contigs were verified and joined together using the addSolexaReads.pl script of the Consed package (Gordon and Green, 2013). The identification of protein-coding genes was carried out following Turmel et al. (2017), whereas tRNAs were identified using tRNA-scan (Lowe and Eddy, 1997) and Arwen (Laslett & Canbäck, 2008). Maps of the organellar genomes were produced using the OGDRAW online server (Lohse et al., 2013).

Maximum Likelihood Phylogenetic Analyses

Two multigene maximum likelihood phylogenies were conducted using the RAxML ver. 8.2.7 (Stamatakis, 2014) software package. Alignments and analytical parameters followed those described in Majewska et al. (2021). One used a 3-gene dataset (*SSU-rbcL-psbC*) as in Majewska et al. (2021) and the other a 7-gene dataset (*SSU-rbcL-psbC-psaA-psaB-psbA-atpB*) as in Theriot et al. (2015). The 3-gene dataset included both *A. micronesica* and *A. vermiculata*, while the 7-gene dataset included only *A. micronesica*, as solely the *rbcL* sequence was available for *A. vermiculata*. All *A. micronesica* genes were obtained from the assembled sequencing reads reported above. In total, 429 and 209 taxa are represented in the 3-gene and 7-gene datasets, respectively. These datasets are available as **Supplementary Data S1, S2**.

RESULTS

Type Species of the *Amicula* Genus

Family: Diploneidaceae

Genus: *Amicula* Witkowski, Lange-Bertalot & Metzeltin

Type species: *Amicula specululum* (Witkowski) Witkowski in Witkowski et al., 2000

Syn.: *Navicula specululum* Witkowski 1994, *Navicula nolens* Simonsen 1959 nom. inval., *Navicula nolens* Simonsen in Hinz et al., 2012

Frustules small, rectangular, relatively broad girdle composed of a few plain, open copulae. Valves elliptic to linear elliptic with broadly rounded apices, 5–9 μ m long, 3–4 μ m in width. Raphe short, straight with slightly expanded external central endings. External apical raphe ends slightly expanded, terminating prior to apices. Transapical striae arranged as a peripheral ring of single areolae along the valve margin, 30–32 in 10 μ m. Each elliptic areola occluded by two rows of perforations.

Geographic distribution: *Amicula specululum* has been recorded from a broad range of habitats. Although the first described specimen originated from brackish waters of the Baltic Sea (ca. 7–8 psu), the species has also been documented in Florida by SEM (Navarro 1982; current study). Furthermore, it has been observed along the Kenya coast in Indian Ocean (Witkowski et al., 2000) and as an endosymbiont in the foraminiferan *Pararotalia calcariformata* from the Eastern Mediterranean Sea; however, the later endosymbiont was misidentified as *Diploneis* sp. (Schmidt et al., 2018, **Figure 4:23**). As identified and illustrated by Nevrova & Petrov 2019, **Figure 4:30**, the *Amicula specululum* specimen they isolated from the Black Sea appears to be *A. vermiculata* instead of *A. specululum*; solving its exact identity requires further study. Note that the presence of *A. specululum* in the Black Sea and in the Lagebaan Lagoon West Coast of South Africa has been confirmed in a separate study (Witkowski, unpublished results).

New Species

Amicula micronesica Lobban, Ashworth & Witkowski sp. nov.

Frustules with two chloroplasts, rectangular in girdle view with a few broad, unperforated open copulae. Valves broadly elliptical (smaller valves, **Figure 3E**) to linear elliptical (larger valves, **Figure 3A**) with broadly rounded apices, 3.2–9.8 μ m long, 2.5–3.7 μ m in width (n=15). Valve face flat at middle to slightly sloping towards mantle. Mantle very narrow and structureless. Raphe sternum externally not differentiated from valve face. Raphe branches straight and short; apical raphe ends slightly expanded, terminating prior to apices. Central raphe ends simple. Internal raphe sternum slightly elevated. Raphe branches with simple central raphe ends terminating in a small and indistinct helictoglossa at apices. Transapical striae developed marginally as single parallel row of elongated areolae, becoming radiate towards apices, 35–36 in 10 μ m. Areolae externally occluded by cribra with digitate projections from areola walls and apparently hymenate occlusions internally.

Differential diagnosis: differing from *A. specululum* and *A. vermiculata* in very small sizes (<10 μ m) and character of the areolae and from *A. specululum* in coarser stria density, 30–32 in

10 μm (Table 1). The shape of the cribrate occlusions differs among the three species, as those of *A. speculum* generally have two rows of perforations (Figure 1H) and those of *A. vermiculata* have vermiculate cribra (Figure 2C), while *A. micronesica* has digitate projections (Figure 3G).

Holotype: Slide ANSP-GC20110 designated here (Figure 3B), Academy of Natural Sciences at Drexel University, Philadelphia, USA, accession ANSP-GC20110

Isotype: slide SZCZ 28139 deposited in Diatom Collection of Andrzej Witkowski, Institute of Marine and Environmental Sciences, University of Szczecin, Szczecin, Poland

Type habitat: microalgal biofilm on sandy sediment surface, ca. 8 m depth, Guam, Piti Municipality, Apra Harbor, "Outhouse Beach" (13° 27' 12" N, 144° 39' 12.56" E), collected May 10, 2015 by C.S. Lobban and M. Scheffer.

Etymology: the species name refers to the Micronesian region of the Western Pacific, hence "micronesica".

Registration: Phycobank <http://phycobank.org/103161>

Geographic distribution: known so far only from the type habitat in Guam.

Molecular markers: partial *SSU* (ON453966), *rbcL* (GenBank: MW324582) and *psbC* (GenBank: MW324636) genes, complete mitochondrial (GenBank: ON390794) and plastid (GenBank: ON390793) genomes.

Amicula vermiculata Chunlian Li, Wachnicka, Frankovich & Witkowski sp. nov.

Valves elliptical to narrowly elliptical with broadly rounded apices, 5.6–9.8 μm long, 3.1–3.8 μm wide. Raphe composed of two short branches. Internal central raphe ends simple, external central raphe ends slightly expanded. External apical raphe ends slightly expanded, terminating prior to apices. Internal apical raphe ends in small, indistinct helictoglossae at

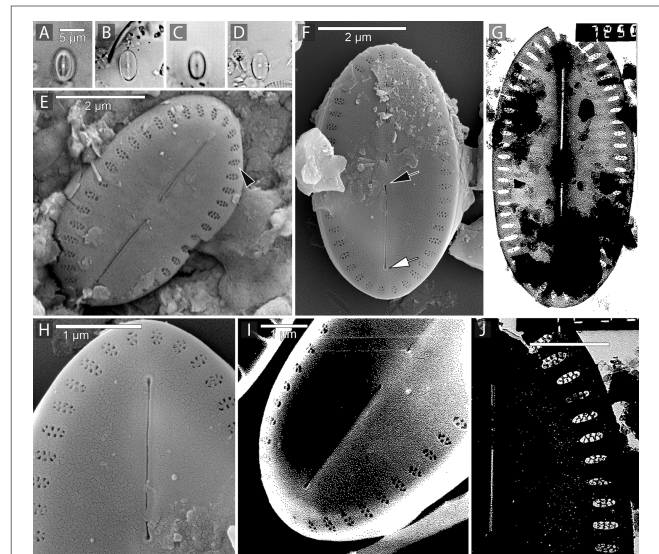


FIGURE 1 | *Amicula speculum* (Witkowski) Witkowski, Lange-Bertalot & Metzeltin the generitype of the genus. Figures (A–D). Light microscopic images of *Amicula speculum* from the type habitat in Puck Bay, Southern Baltic Sea. Figures (E, F, H, I). SEM images illustrating the valve exterior. Figures (G, J). TEM images from Puck Bay. Figures (F, H). specimens from the Western Baltic Sea. Figure (E). Specimen with well-developed cribrate areolae (black arrowhead). Note the short raphe branches and relatively large central nodule. Figures (F, H). Valve exterior with central raphe ending (black arrow) and apical raphe ending (white arrow). Figures (G, J). Cribrate areolae and short raphe branches illustrated in TEM

apices. Raphe sternum slightly elevated internally. Transapical striae arranged as a peripheral ring of single areolae along the valve margin, occluded externally by vermiculate cribra and apparently hymenate occlusions internally, 28–32 in 10 μm .

TABLE 1 | Comparison table between the three species of the genus *Amicula*.

		<i>Amicula speculum</i>	<i>Amicula micronesica</i>	<i>Amicula vermiculata</i>
Dimensions	Length	5.0 - 9.0	3.2 - 9.8	5.6 - 9.8
	Width	3.0 - 4.0	2.5 - 3.7	3.1 - 3.8
Frustule		small, rectangular in gridle view	rectangular in gridle view, valve face flat at the middle to slightly sloping towards mantle	small, rectangular in gridle view
Valve outline		elliptic to linear elliptical	broadly elliptical to linear elliptical	elliptical to narrowly elliptical
Girdle		broad, composed of few plain copulae	broad, plain, open copulae	ND
Apices		broadly rounded	broadly rounded	broadly rounded
Raphe		short, straight	short, straight	short, straight
Raphe endings	Internal central	ND	simple	simple
	External central	slightly expanded	simple	slightly expanded
	Internal apical	ND	simple with small, indistinct helictoglossae	terminating prior to the apices with small, indistinct helictoglossae
	External apical	slightly expanded, terminating prior to the apices	slightly expanded, terminating prior to the apices	slightly expanded, terminating prior to the apices
	Raphe sternum		slightly elevated internally	slightly elevated internally
Striae arrangement		as peripheral ring of single elliptic areolae along the valve margin	as peripheral ring of single elongated areolae along the valve margin	as peripheral ring of single areolae along the valve margin
Striae in in 10 μm		30 - 32	35 - 36	28 - 32
Areolae occlusions	Internally	ND	hymenate occlusion	hymenate occlusion
	Externally	two rows of perforations	cribra with digitate projections from areola walls	vermiculate cribra

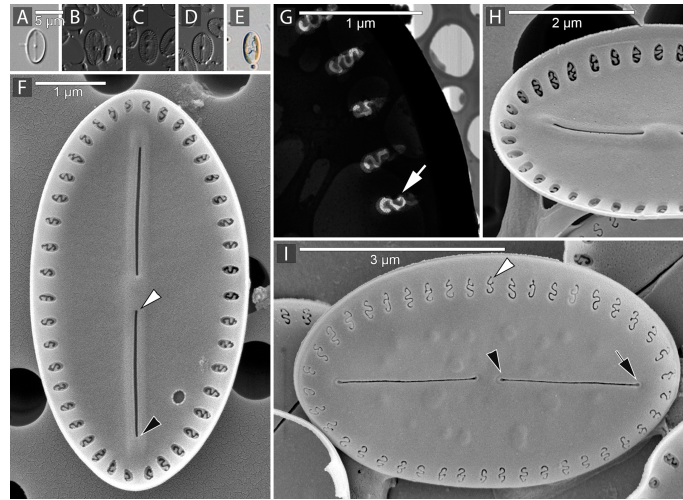


FIGURE 2 | *Amicula vermiculata* Chunlian Li, Frankovich, Wachnicka & Witkowski sp. nov. Figure (A). Light microscopic image of a wild specimen of *A. vermiculata*. Figures (B–D). LM image of the specimens from culture (strain SZCZCH282). Specimen in Figure (D) is selected as the holotype. Figure (E) is a live specimen from the culture. Figures (F, H, I). SEM images of *A. vermiculata*. Figure (G). Close up of *A. vermiculata* from culture imaged with TEM. Figure (F). Internal view of a specimen from natural sample. Note the internal raphe branches with internal central raphe end (white arrowhead) and apical raphe end with very small helictoglossa (black arrowhead). Figure (G). Close up of the internal valve view illustrating the hyemate areola occlusion (white arrow). Figure (H). Internal view of the specimen from the culture. Figure (I). External view of the specimen from culture; note the cribrate areola occlusions (white arrowhead) and the short raphe branches with external central raphe ends (black arrowhead) and external apical raphe end (black arrow).

Differential diagnosis: differing from congeners in the vermiculate external areolar openings and from *A. micronesica* also in coarser stria density (Table 1).

Holotype: Slide No.: #MKA 330 designated here (Figure 2D) deposited in Academy of Natural Sciences at

Drexel University, Philadelphia, USA, accession number ANSP-GC59349

Isotype: slide SZCZCH282 deposited in Diatom Collection of Andrzej Witkowski, Institute of Marine and Environmental Sciences, University of Szczecin, Szczecin, Poland

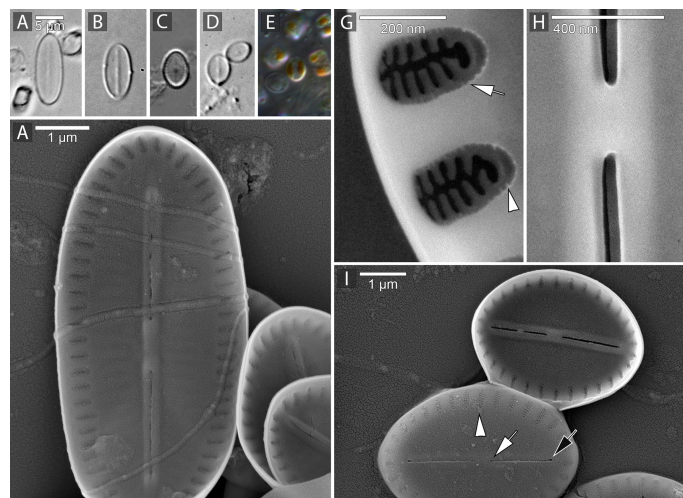
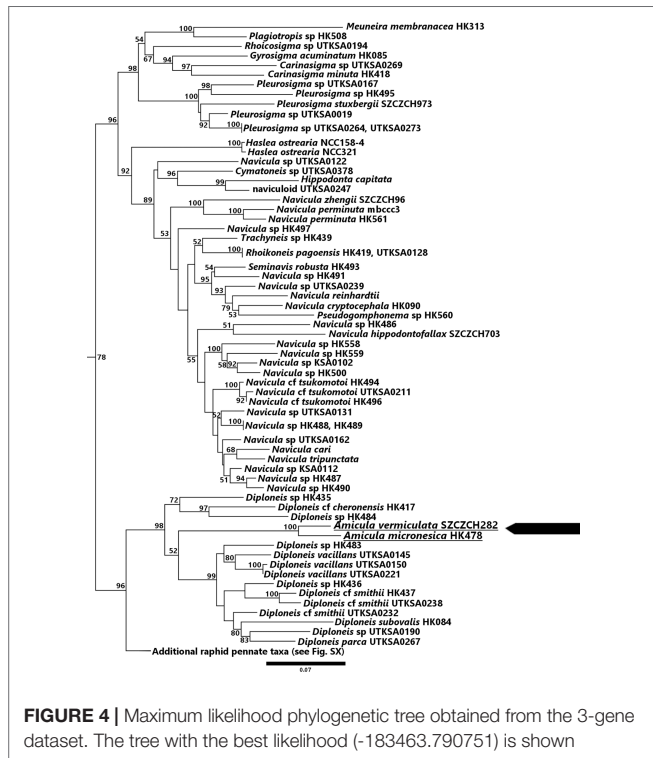


FIGURE 3 | *Amicula micronesica* Lobban, Ashworth & Witkowski sp. nov. Figures (A–D). Light microscopic images of *A. micronesica* from the holotype slide, holotype specimen in Figures (B, E) Specimen of *A. micronesica* from the culture with two plastids. Figures (F–I). Specimens of *A. micronesica* illustrated in SEM. Figure (F) Specimen illustrating valve internal view with relatively short raphe branches and relatively large central nodule. Figure (G) Internal valve view illustrating the cribrate areola (white arrow) and remnants of the hyemate internal occlusions (white arrowhead). Figure (H) close up of the internal central raphe endings. Figure (I) Internal and external valve view note the external view of the areola occlusions (white arrowheads), the central external raphe end (white arrow) and external apical raphe end distant from the valve apex (black arrow).



Type habitat: Marquesas Keys (24° 40' 53" N, 82° 19' 51" W) on sediment from benthic grab sample, water depth = 20 m, sampled on February 15, 2013.

Etmology: species name is derived from the vermiculate shape of the cribra, hence “vermiculata”

Registration: Phycobank <http://phycobank.org/103162>

Geographic distribution: observed in the type habitat; not rare. It was also observed in Maria La Gorda (Western Cuba) in SEM (A. Witkowski unpublished observation)

Molecular markers: partial *rbcL* gene (GenBank: ON390792).

Molecular Phylogeny

The maximum likelihood phylogenies that were inferred using the 3-gene and 7-gene datasets both suggest a close relationship between *Amicula* and *Diploneis* (Figures 4, 5, respectively). The 7-gene phylogeny resolves *A. micronesica* as sister to *Diploneis subovalis* with 100% bootstrap support (bs), though it should be noted these taxa are the only representatives of their respective genera. In the same phylogeny, the *Diploneis*+*Amicula* clade is sister to a clade of *Fallacia*+*Pinnularia*+*Caloneis*, but this relationship is poorly supported (<50% bs). In the analysis of the 3-gene dataset with increased taxon sampling, however, the genus *Diploneis* is polyphyletic with respect to the *A. micronesica* and *A. vermiculata* clade. A clade of three *Diploneis* taxa (HK417, HK435, HK484; bs = 87%) is sister to *Amicula* plus the remaining *Diploneis* taxa in the dataset, but this relationship is weakly supported (bs = 54%). The complete trees are available as **Supplementary Data S3** (3-gene tree) and **S4** (7-gene tree).

Plastid Genome of *Amicula micronesica*

The *A. micronesica* plastid genome is 179134-bp long and features the typical quadripartite architecture found in other diatom plastomes (GenBank: ON390793) (Figure 6). The 80166-bp large single-copy region contains 67 protein coding genes, 18 non-conserved open-reading frames (ORF) and 17 tRNA genes, whereas the 41046-bp small single-copy region encodes 51 proteins and 6 tRNAs (Table 2). The 28961-bp inverted repeat region is gene-rich, comprising 10 protein-coding, 3 rRNA and 4 tRNA genes in addition to 12 non-conserved ORFs (Table 2). Interestingly, this region features the *acpP* gene that encodes a putative 80 amino-acid protein containing all the conserved domains of an acyl-carrier protein. (Yu et al., 2018). The *A. micronesica* genome also displays the *bas1*, *syfB*, *thiG* and *thiS* genes, which are often absent or present as pseudogenes in other diatom plastomes. However, the *tsf* gene was not identified.

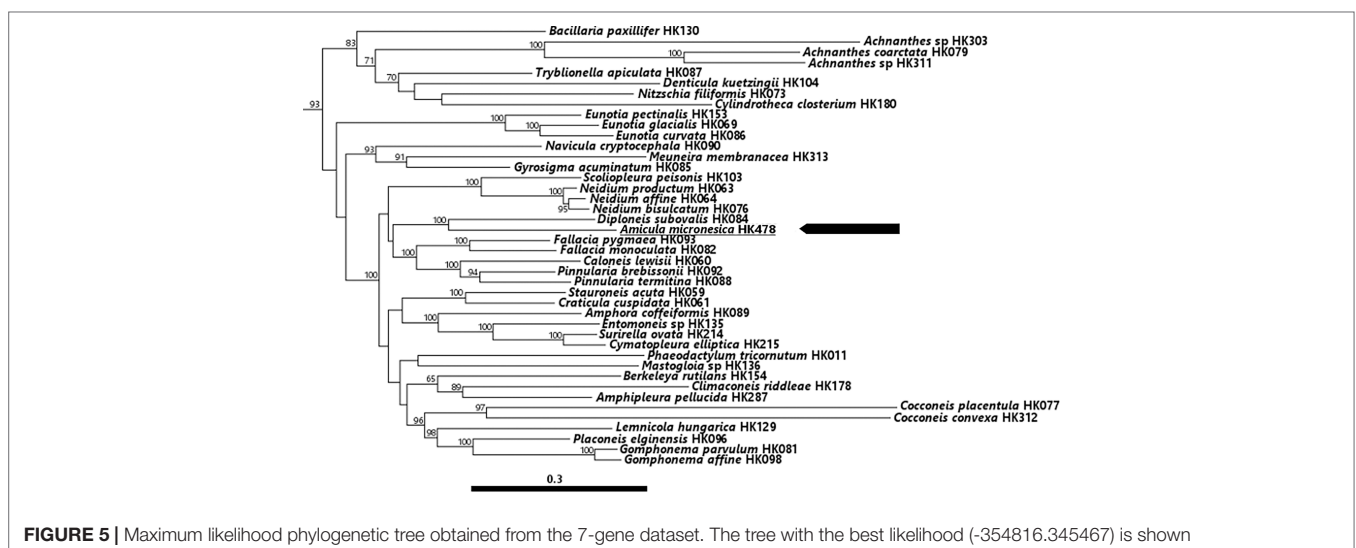


TABLE 2 | Gene composition of the inverted repeat (IR) and single-copy regions (large, LSU; small, SSU) of the *Amicula micronesica* plastid genome.

LSC	<i>orf680a, orf154b, orf160b, orf136a, orf273a, orf171a, psaB, psaA, psaJ, psaF, psbI, ycf41, ycf39, cbbX, psaL, petL, ycf4, tRNA-Gly, tRNA-Gly, psbE, psbF, psbL, psbJ, ycf90, tRNA-Gly, psbZ, ycf12, tRNA-Lys, psbC, psbD, psal, psbK, petG, tRNA-Thr, tRNA-Arg, tRNA-Val, tRNA-Tyr, ycf33, tRNA-Met, tRNA-Ser, tRNA-Asp, petM, petN, psbH, psbN, psbT, psbB, rps14, psaM, chlI, secG, petD, petB, tRNA-Ser, psaD, tRNA-Met, rpl12, rpl1, rpl11, tRNA-Trp, dnaB, psbX, ycf66, psbV, tRNA-Arg, tRNA-Met, rpl19, petF, petA, tatC, atpE, atpB, ycf3, rps18, rpl33, rps20, rpoB, rpoC1, rpoC2, rps2, rbcS, rbcL, sufB, sufC, atpI, atpH, atpG, atpF, atpD, atpA, orf166a, orf179c, orf168b, orf127a, orf179a, orf149a, orf229a, orf317a, orf186a, orf513a, orf310a, orf293a</i>
SSC	<i>rbcR, rpl21, rpl27, secA, rpl34, ycf46, ccs1, psbA, ccsA, clpC, tRNA-Cys, tRNA-Leu, rps16, rps4, tRNA-His, thiS, syfB, psb28, tRNA-Gln, tRNA-Arg, groEL, dnaK, rpl3, rpl4, rpl23, rpl2, rps19, ycf88, rpl22, rps3, rpl16, rpl29, rps17, rpl14, rpl24, rpl5, rps8, rpl6, rpl18, rps5, secY, rpl36, rps13, rps11, rpoA, rpl13, rps9, rpl31, rps12, rps7, tufA, rps10, rps6, tRNA-Asn, thiG, psaC, psbY</i>
IR	<i>orf156, ftsH, psaE, bas1, rpl35, rpl20, ycf45, acpP, orf263, orf140, orf102, orf158, tRNA-Pro, ycf89, orf135, ms, tRNA-Ile, tRNA-Ala, ml, rm5, orf162, orf129, orf371, orf110, orf164, orf126, ycf35, rpl32, tRNA-Leu</i>

Mitochondrial Genome of *Amicula Micronesica*

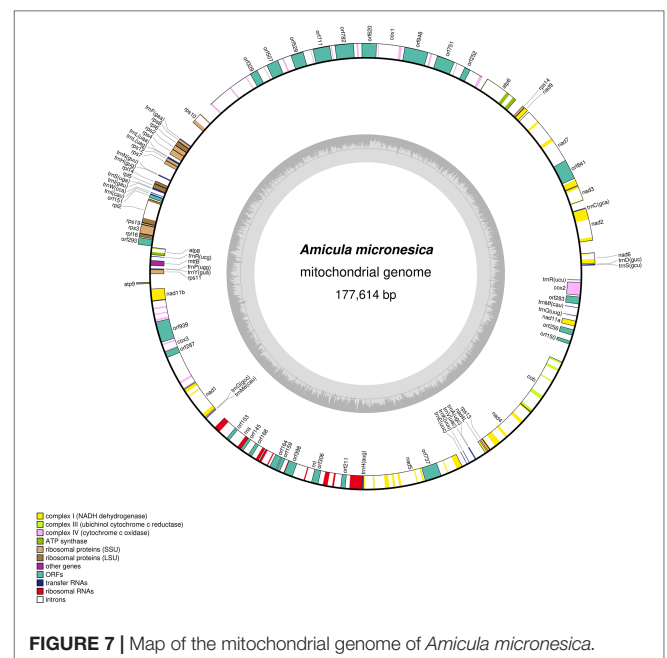
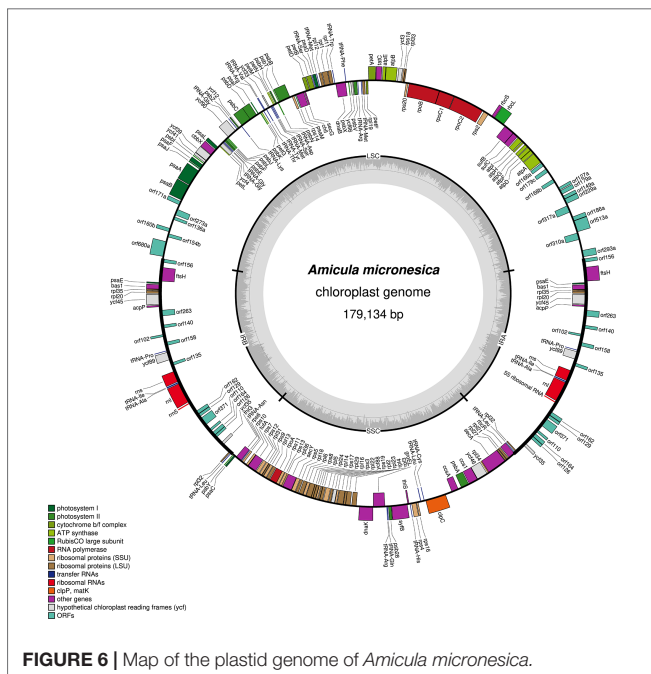
The *A. micronesica* mitogenome (GenBank: ON390794) has a minimum size of 177614 bp (Figure 7). Its size is most probably larger, considering that the presence of tandem repeats at both ends of the linear genome sequence prevented the circularization of the DNA molecule during assembly.

for clarity, the mitogenome is being displayed as complete and circular on Figure 7. The 57 introns identified in the genome (Supplementary Data S5), all belonging to the group II intron family, account for 113645 bp, i.e., 64% of the genome size. With a total of 12 introns, the 36416-bp *cox1* is the most intron-rich gene.

The *A. micronesica* mitogenome contains 35 conserved protein-coding genes. Although the conserved *orf151* (Pogoda et al., 2018) is included within this set of genes, it is located between *rpl2* and *rpl5* rather than in the ubiquitous *tatC-orf157-rps11* cluster originally described by Pogoda et al. (2018). In addition to the conserved ORFs, 25 non-conserved ORF were annotated, 20 of which code for putative group II intron reverse transcriptases (RT) and/or maturases.

The *A. micronesica* mitogenome was annotated using the genetic code 4, instead of the universal code 1. Use of the latter code caused the appearance of several premature TGA stop codons within four conserved protein-coding genes (*mttB* (also known as *tatC*), *nad2*, *rps10* and *rps11*), as well as in six intron-encoded ORFs. The latter ORFs and their products (in parentheses) consist of *orf145* in *rns* (RT), *orf164* in *rnl* (RT), *orf306* in *rnl* (RT/maturase), *orf751* in *cox1* (RT/maturase), *orf841* in *nad7* (RT/maturase), and *orf948* in *cox1* (RT/HNH endonuclease).

Among the 25 tRNA genes identified with tRNAscan in the *A. micronesica* mitogenome, none was found to encode the tRNA-Trp(*uca*) required to decode UGA codons as Trp. Analysis with ARWEN returned two additional tRNA genes with very degenerated secondary structures: one resides within *cox3* and codes for a 60-bp tRNA with a 6-bp TV-loop and no D-loop, whereas the other resides in a non-coding region and codes for 63-bp tRNA lacking the TV-loop.



DISCUSSION

Taxonomy

In the original description of *Amicula*, the classification of the genus within the Bacillariophyceae was not explicitly stated by the authors (Witkowski et al., 2000). Later, Cox (2015) included *Amicula* in the Order Naviculineae Hendey and listed it among a number of genera, mentioning that the positions of these genera among Naviculales are uncertain. Both maximum likelihood phylogenies inferred in our study placed *Amicula* among the Diploneidinae D.G. Mann and the Family Diploneidaceae D.G. Mann. *Amicula* is thus far the third genus reported in this family next to *Diploneis* (C.G. Ehrenberg) P.T. Cleve and the extinct genus *Raphidodiscus* H.L. Smith in T. Christian.

Due to the scarcity of distinctive morphological characters for *Amicula*, a search for characters shared between the two extant genera of the family is not easy but remains possible. In the most recent monograph on freshwater *Diploneis*, Lange-Bertalot et al. (2020) point out longitudinal canals as prominent character of the latter genus (cf. also Droop, 1998 for marine taxa). While these longitudinal canals are missing in *Amicula*, the two genera share a type of cribrate occlusion in exterior of the areolae and hymenate occlusions on the valve internal surface (Round et al., 1990, Lange-Bertalot et al., 2020). Interestingly, some freshwater *Diploneis* taxa possess cribra in the poroids along the longitudinal canal which strongly resemble the vermiculate cribra in *A. vermiculata* (Lange-Bertalot et al., 2020). Marine species related to *Diploneis sejuncta* (Schmidt) Jørgensen exhibit cribrate areola occlusions with hymenate internal membranes, which are similar to the “vermiculate” cribra illustrated here in *Amicula* (Droop, 1998). Droop (1998) considered this group of taxa an ancient lineage based on the striae separating the longitudinal canal from the raphe sternum, a character not observed in other *Diploneis* taxa. In his article, Droop (1998) reported those taxa related to *D. sejuncta* as extremely rare, suggesting that testing this hypothesis by molecular phylogenetic studies might be difficult if material cannot be located for cultures and DNA extraction. Yet, in our recent assessment of diatom biodiversity, these taxa were abundant in the coral reef habitats from Florida (Frankovich, unpublished observations) and Indonesia (Risjani et al., 2021).

A Complex Mitogenome

In addition to the taxonomic description of *Amicula micronesica*, we also described its organellar genomes, which include the largest mitogenome (177614 bp) found so far among stramenopiles. Diatom mitogenomes generally range from 32777 bp (in *Melosira undulata*) and 77356 bp (in *Phaeodactylum tricornerutum*) (Pogoda et al., 2018). Aside from the *Amicula* mitogenome, only two other diatom mitogenomes are known to exceed 100 kb: the 103605-bp mitogenome of *Halamphora caladilacuna* Stepanek and Kocielek, 2018 (Pogoda et al., 2018) and the yet undescribed 107979-bp mitogenome of *Fragilaria crotonensis* Kitton, 1869 (GenBank: JAKSYS010000135). The remarkable size of the *A. micronesica* mitogenome is clearly the result of massive invasion of group II introns at multiple sites within coding regions. Similarly, a large part of the increased size of the *H. caladilacuna*

mitogenome can be explained by the proliferation of group II introns. In the latter genome, 21 group II introns are inserted in eight different genes, namely *cox1* (8 introns), *cox2* (1 intron), *cox3* (1 intron), *cob* (1 intron), *rps2* (1 intron), *nad7* (1 intron), *rrl* (5 introns) and *rrs* (3 introns). In the *A. micronesica* mitogenome, a total of 57 introns are inserted in 17 genes that include all those listed above for *H. caladilacuna*, except *rps2*. By comparison, all other diatom mitogenomes available in public databases contain much fewer introns and these are restricted to *cox1*, *rrl* and *rrs* (Pogoda et al., 2018).

A third of the *A. micronesica* group II introns (nine in *cox1*, three in *rrl*, two in *cox3* and *rns*, and one in *nad5* and *nad7*) potentially encode proteins with reverse transcriptase, intron maturase, and/or HNH-endonuclease domains. These proteins may assist intron splicing and enable introns to integrate at cognate sites in intronless genes (Lambowitz and Belfort, 2015). In addition, they may facilitate the spread of group II introns at noncognate sites within the same genome (Lambowitz and Belfort, 2015). Only a few cases of intragenomic proliferation of group II introns have been previously documented for organelles. Such evidence has been reported for the chloroplasts in chlorophyte green algae (Brouard et al., 2016; Turmel et al., 2016), euglenids (Hallick et al., 1993; Pombert et al., 2012; Bennett and Triemer, 2015) and the red alga *Porphyridium purpureum* (Perrineau et al., 2015).

Another interesting feature of the *A. micronesica* mitogenome is the use of genetic code 4 for translation. This is not the first time this code is documented for diatoms. It was previously reported for the first species whose mitogenome had been sequenced, namely *Thalassiosira pseudonana* Hasle & Heimdal 1970 (Oudot-Le Secq and Green, 2011). *T. pseudonana* is a Mediophycean species, and as such is genetically distant from the Bacillariophyceae. In contrast to the mitogenome of *A. micronesica*, the *T. pseudonana* mitogenome contains a functional *trnW(tca)* gene that codes for a tRNA-Trp(*uca*) capable of decoding the UGA codon. Sequencing of microalgal mitogenomes sometimes leads to the discovery of deviant, new genetic codes (Turmel et al., 2019) often involving the reading of the UGA codon as tryptophan instead of a stop codon (Turmel et al., 2010; Turmel et al., 2020). A list of deviant genetic codes in microalgal mitogenomes can be found in Noutahi et al. (2019).

At this stage, four hypotheses can be proposed to explain the lack of a mitochondrial-encoded tRNA-Trp(*uca*) in *A. micronesica*. First, it is possible that the missing tRNA gene resides in the non-assembled portion of the mitogenome. As stated above, the complete mitogenome of *A. micronesica* could be larger than the assembled linear genome sequence, likely due to the presence of tandemly repeated sequences at the extremities of this sequence. A second hypothesis would be that the degenerated tRNA entirely missing the TV-loop, which was detected using ARWEN, could be functional. However, although non-standard forms of mitochondrial tRNA can be found among metazoans (Krahn et al., 2020), they are rather scarce among protists (Gray et al., 1998). A third hypothesis would be that a functional tRNA-Trp(*uca*) is imported from the cytosol. The need of tRNA importation among microalgae has been suspected for a long time among species of the genus *Chlamydomonas* (Gray et al., 1998). Finally, it is possible that the tRNA-Trp(*cca*)

of *A. micronesica* undergoes post-transcriptional modification of its anticodon arm, allowing it to recognize both UGG and UGA codons. Such a mechanism was suggested to explain the use of code 4 in the mitogenome of *Pycnococcus provasolii* (Turmel et al., 2010).

Unfortunately, a complete mitogenome sequence is not currently available for *A. vermiculata*. Therefore, we cannot assess nor predict if the distinctive features described in this study are shared between species of *Amicula*. With regards to the number of introns, earlier reports have shown that their number is strongly variable among species of the same genus (Pogoda et al., 2018) and even among populations of the same species (Gastineau et al., 2021). Interestingly, with 299 taxonomically accepted species, *Diploneis*, the sister genus to *Amicula*, is a far more speciose genus (Guiry and Guiry, 2022). Comparing the mitogenomes of the diverse *Diploneis* and species-depauperate *Amicula* would provide an interesting comparative dataset to investigate how different diversification rates in closely related genera have shaped organellar genomes during evolution.

DATA AVAILABILITY STATEMENT

The datasets presented in this study can be found in online repositories. The names of the repository/repositories and accession number(s) can be found below: <https://www.ncbi.nlm.nih.gov/genbank/>, ON453966, MW324582, MW324636, ON390794, ON390793, ON390792.

AUTHOR CONTRIBUTIONS

Sampling and isolation were performed by CLL, MA, AWi, TF, AWa, EG, CSL, PD, AB. Scanning electron microscopy was performed by MA, AWi, TF, CSL. Administration of the project was the responsibility of AWi and CL. Barcoding and phylogenies were done by MA and ET. Genomic analyses were performed by RG, MT, CL and CO. Writing the original draft was done by RG. All authors participated in manuscript revision. All authors contributed to the article and approved the submitted version.

REFERENCES

- Alverson, A. J., Jansen, R. K., and Theriot, E. C. (2007). Bridging the Rubicon: Phylogenetic Analysis Reveals Repeated Colonizations of Marine and Fresh Waters by Thalassiosiroid Diatoms. *Mol. Phylogenet. Evol.*, 45 (1), 193–210. doi: 10.1016/j.ympev.2007.03.024
- Bankevich, A., Nurk, S., Antipov, D., Gurevich, A., Dvorkin, M., Kulikov, A. S., et al. (2012). SPAdes: a new genome assembly algorithm and its applications to single-cell sequencing. *J. Comput. Biol.* 19, 455–477. doi: 10.1089/cmb.2012.0021
- Bennett, M. S. and Triemer, R. E. (2015). Chloroplast genome evolution in the Euglenaceae. *J. Eukaryot. Microbiol.* 62, 773–785. doi: 10.1111/jeu.12235
- Brouard, J. S., Turmel, M., Otis, C. and Lemieux, C. (2016). Proliferation of group II introns in the chloroplast genome of the green alga *Oedocladium carolinianum* (Chlorophyceae). *PeerJ* 4, e2627. doi: 10.7717/peerj.2627
- Cox, E. J. (2015). "Diatoms, Diatomeae (Bacillariophyceae s.l., Bacillariophyta)," in *Syllabus of Plant Families. Adolf Engler's Syllabus of Plant Families*. Ed. Frey, W. (Stuttgart: Germany Borntraeger), 64–103.

FUNDING

Sampling in Marquesas, Florida and research on isolated Florida strain have been funded from National Science Centre in Cracow, Poland within the frame of the project: 2012/04/S/ST10/00017 granted to AWa and 2017/25/N/ST10/01729 granted to AB. The project also benefited from the support of the European Commission under the Horizon 2020 Research and Innovation Program GHANA (The Genus Haslea, New marine resources for blue biotechnology and Aquaculture, grant agreement No (734708/GHANA/H2020-MSCA-RISE-2016) J.-L.M.) and also the 2017–2022 research funds granted for implementation of a co-financed international research project from the Polish Ministry of Science and Higher Education. This work was supported by the Natural Sciences and Engineering Research Council of Canada under Grant RGPIN-2017-04506.

ACKNOWLEDGMENTS

Friedel Hinz and Bank Beszteri are greatly acknowledged for sharing with us SEM images of *Navicula nolens* Simonsen. Dr. Mateusz Rybak from University of Rzeszów and Dr. Tomasz Płociński from Warsaw University of Technology are acknowledged for their help with Scanning Electron Microscope and Transmission Electron Microscope respectively. The authors also thank Tom Beasley for his generous assistance with electron microscopy at the Florida Center for Analytical and Electron Microscopy at Florida International University. This is contribution #1443 from the Institute of Environment, Florida International University.

Supplementary Material includes Supplementary Data S1 (3-gene dataset), S2 (7-gene dataset), S3 (full 3-gene tree), S4 (full 7-gene tree) and S5 (list of the introns in the mitogenome).

SUPPLEMENTARY MATERIAL

The Supplementary Material for this article can be found online at: <https://www.frontiersin.org/articles/10.3389/fmars.2022.941506/full#supplementary-material>

- Cox, T. E., Cebrian, J., Tabor, M., West, L. and Krause, J. W. (2020). Do diatoms dominate benthic production in shallow systems? A case study from a mixed seagrass bed. *Limnol. Oceanogr. Lett.* 5, 425–434. doi: 10.1002/lo2.10167
- Doyle, J. J. and Doyle, J. L. (1990). Isolation of plant DNA from fresh tissue. *Focus* 12, 13–15.
- Droop, S. J. M. (1998). *Diploneis sejuncta* (Bacillariophyta) and some new species from an ancient lineage. *Phycologia* 37, 340–356. doi: 10.2216/i0031-8884-37-5-340.1
- Field, C. B., Behrenfeld, M. J., Randerson, J. T., and Falkowski, P. (1998). Primary Production of the Biosphere: Integrating Terrestrial and Oceanic Components. *Science* (New York, N.Y.), 281(5374), 237–240. doi: 10.1126/science.281.5374.237
- Gastineau, R., Hansen, G., Poulin, M., Lemieux, C., Turmel, M., Bardeau, J.-F., et al. (2021). *Haslea silbo*, A Novel Cosmopolitan Species of Blue Diatoms. *Biology* 10 (4), 328. doi: 10.3390/biology10040328
- Gordon, D. and Green, P. (2013). Consed: a graphical editor for next-generation sequencing. *Bioinformatics* 29, 2936–2937. doi: 10.1093/bioinformatics/btt515
- Gray, M. W., Lang, B. E., Cedergren, R., Golding, G. B., Lemieux, C., Sankoff, D., et al. (1998). Genome structure and gene content in protist mitochondrial DNAs. *Nucleic Acids Res.* 26 (4), 865–878. doi: 10.1093/nar/26.4.865

- Guillard, R. R. L. (1975). "Culture of phytoplankton for feeding marine invertebrates", 26–60. in *Culture of Marine Invertebrate Animals*. Eds. Smith, W. L. and Chanley, M. H. (New York, USA: Plenum Press)
- Guiry, M. D. and Guiry, G. M. (2022) *AlgaeBase. World-wide electronic publication* (Galway: National University of Ireland). Available at: <https://www.algaebase.org> (Accessed May 6, 2022).
- Hallick, R. B., Hong, L., Drager, R. G., Favreau, M. R., Monfort, A., Orsat, B., et al. (1993). Complete sequence of *Euglena gracilis* chloroplast DNA. *Nucleic Acids Res.* 21, 3537–3544. doi: 10.1093/nar/21.15.3537
- Hinz F., Simonsen R. and Crawford R. M. (2012). Validation of 42 Names of Diatom Taxa From the Baltic Sea, *Diatom Research*, 27(2), 81–89, doi: 10.1080/0269249X.2012.687562
- Houki, S., Kawamura, T., Ogawa, N., and Watanabe, Y. (2018). Efficient Crushing of Hard Benthic Diatoms in the Gut of the Manila Clam *Ruditapes philippinarum*—Experimental and Observational Evidence. *Journal of Experimental Marine Biology and Ecology*, 505, 35–44, doi: 10.1016/j.jembe.2018.04.007
- Krahn, N., Fischer, J. T. and Söll, D. (2020). Naturally Occurring tRNAs With Non-canonical Structures. *Front. Microbiol.* 11. doi: 10.3389/fmicb.2020.596914
- Lambowitz, A. M. and Belfort, M. (2015). Mobile Bacterial Group II Introns at the Crux of Eukaryotic Evolution. *Microbiol. Spectr.* 3, MDNA3-0050-2014. doi: 10.1128/microbiolspec.MDNA3-0050-2014
- Lange-Bertalot, H., Fuhrmann, A. and Werum, M. (2020). "Freshwater Diploneis: species diversity in the Holarctic and spot checks from elsewhere," in *Diatoms of Europe*, vol. 09. Ed. Lange-Bertalot, H. (Glashütten, Germany: Koeltz Botanical Book), 526 pp.
- Laslett, D. and Canbäck, B. (2008). ARWEN, a program to detect tRNA genes in metazoan mitochondrial nucleotide sequences. *Bioinformatics* 24, 172–175. doi: 10.1093/bioinformatics/btm573
- Lohse, M., Drechsel, O., Kahlau, S. and Bock, R. (2013). OrganellarGenomeDRAW—a suite of tools for generating physical maps of plastid and mitochondrial genomes and visualizing expression data sets. *Nucleic Acids Res.* 41, W575–W581. doi: 10.1093/nar/gkt289
- Lowe, T. M. and Eddy, S. R. (1997). tRNAscan-SE: a program for improved detection of transfer RNA genes in genomic sequence. *Nucleic Acids Res.* 25, 955–964. doi: 10.1093/nar/25.5.955
- Majewska, R., Ashworth, M. P., Bosak, S., Goosen, W. E., Nolte, C., Filek, K., et al. (2021). On Sea Turtle-associated *Craspedostauros* (Bacillariophyta), with Description of Three Novel Species. *J. Phycol.* 57, 199–218. doi: 10.1111/jpy.13086
- Navarro, J. N. (1982). Marine Diatoms Associated with Mangrove Prop Roots in the Indian River, Florida, U. S. A. *Bibliotheca Phycologica*, 61, 1–151.
- Nevrova, E. L. and Petrov, A. (2019). Benthic diatoms species richness at Dvuyakornaya Bay and other coastal sites of Crimea (the Black Sea) under various environments. *Mediterr. Mar. Sci.* 20, 506–520. doi: 10.12681/mms.20319
- Noutahi, E., Calderon, V., Blanchette, M., El-Mabrouk, N. and Lang, B. F. (2019). Rapid Genetic Code Evolution in Green Algal Mitochondrial Genomes. *Mol. Biol. Evol.* 36, 766–783. doi: 10.1093/molbev/msz016
- Oudot-Le Secq, M. P. and Green, B. R. (2011). Complex repeat structures and novel features in the mitochondrial genomes of the diatoms *Phaeodactylum tricorutum* and *Thalassiosira pseudonana*. *Gene* 476, 20–26. doi: 10.1016/j.gene.2011.02.001
- Perrineau, M. M., Price, D. C., Mohr, G. and Bhattacharya, D. (2015). Recent mobility of plastid encoded group II introns and twintrons in five strains of the unicellular red alga *Porphyridium*. *PeerJ* 3, e1017. doi: 10.7717/peerj.1017
- Pogoda, C. S., Keepers, K. G., Hamsher, S. E., Stepanek, J. G., Kane, N. C. and Kocielek, J. P. (2018). Comparative analysis of the mitochondrial genomes of six newly sequenced diatoms reveals group II introns in the barcoding region of *cox1*. *Mitochondrial DNA Part A* 30, 43–51. doi: 10.1080/24701394.2018.1450397
- Pombert, J. F., James, E. R., Janouskovec, J. and Keeling, P. J. (2012). Evidence for transitional stages in the evolution of euglenid group II introns and twintrons in the *Monomorpha aenigmatica* plastid genome. *PLoS One* 7, e53433. doi: 10.1371/journal.pone.0053433
- Risjani, Y., Witkowski, A., Kryk, A., Yunianta, Górecka, E., Krzywda, M., et al. (2021). Indonesian Coral Reef Habitats Reveal Exceptionally High Species Richness and Biodiversity of Diatom Assemblages. *Estuarine, Coastal and Shelf Science*, 261: e107551. doi: 10.1016/j.ecss.2021.107551
- Round, F. E., Crawford, R. M. and Mann, D. G. (1990). *Diatoms: Biology and Morphology of the Genera* (Cambridge: Cambridge University Press).
- Schmidt, C., Morard, R., Romero, R. and Kucera, M. (2018). Diverse Internal Symbiont Community in the Endosymbiotic Foraminifera *Pararotalia calcariformata*: Implications for Symbiont Shuffling Under Thermal Stress. *Front. Microbiol.* 9. doi: 10.3389/fmicb.2018.02018
- Simonsen, R. (1959). Neue Diatomeen aus der Ostsee. I. Kieler Meeresforschungen, 15, 74–83.
- Smol J and Stoermer E. (2010). "The Diatoms: Applications for the Environmental and Earth Sciences," 2nd Edition, Cambridge: Cambridge University Press. doi: 10.1017/CBO9780511763175
- Stamatakis, A. (2014). RAxML version 8: a tool for phylogenetic analysis and post-analysis of large phylogenies. *Bioinformatics* 30, 1312–1313. doi: 10.1093/bioinformatics/btu033
- Theriot, E. C., Ashworth, M. P., Nakov, T., Ruck, E. and Jansen, R. K. (2015). Dissecting signal and noise in diatom chloroplast protein encoding genes with phylogenetic information profiling. *Mol. Phylogenet. Evol.* 89, 28–36. doi: 10.1016/j.ympev.2015.03.012
- Turmel, M., Lopes Dos Santos, A., Otis, C., Sergerie, R. and Lemieux, C. (2019). Tracing the Evolution of the Plastome and Mitogenome in the Chlorophyceae Uncovered Convergent tRNA Gene Losses and a Variant Plastid Genetic Code. *Genome Biol. Evol.* 11, 1275–1292. doi: 10.1093/gbe/evz074
- Turmel, M., Otis, C. and Lemieux, C. (2010). A deviant genetic code in the reduced mitochondrial genome of the picoplanktonic green alga *Pycnococcus provasolii*. *J. Mol. Evol.* 70, 203–214. doi: 10.1007/s00239-010-9322-6
- Turmel, M., Otis, C. and Lemieux, C. (2016). Mitochondrion-to-chloroplast DNA transfers and intragenomic proliferation of chloroplast group II introns in *Gloettilopsis* green algae (Ulotrichales, Ulvophyceae). *Genome Biol. Evol.* 8, 2789–2805. doi: 10.1093/gbe/evw190
- Turmel, M., Otis, C. and Lemieux, C. (2017). Divergent copies of the large inverted repeat in the chloroplast genomes of ulvophycean green algae. *Sci. Rep. UK* 7 (1), 994. doi: 10.1038/s41598-017-01144-1
- Turmel, M., Otis, C., Vincent, A. T. and Lemieux, C. (2020). The complete mitogenomes of the green algae *Jenufa minuta* and *Jenufa perforata* (Chlorophyceae, *incertae sedis*) reveal a variant genetic code previously unrecognized in the Chlorophyceae. *Mitochondrial DNA Part B* 5, 1516–1518. doi: 10.1080/23802359.2020.1742229
- Witkowski, A. (1994). Recent and Fossil Diatom Flora of the Gulf of Gdansk, Southern Baltic Sea. *Origin, composition and changes of diatom assemblages during the Holocene. Bibliotheca Diatomologica*, 28, 312.
- Witkowski, A., Lange-Bertalot, H. and Metzeltin, D. (2000). "Diatom Flora of Marine Coasts I," in *Iconographia Diatomologica. Annotated Diatom Micrographs*, vol. Vol. 7. Ed. Lange-Bertalot, H. (Königstein, Germany: Koeltz Scientific Books). Diversity-Taxonomy-Identification.
- Yu, M., Ashworth, M. P., Hajrah, N. H., Khiyami, M. A., Sabir, M. J., Alhebshi, A. M., et al. (2018). Evolution of the plastid genomes in diatoms. *Adv. Bot. Res.* 85, 129–155. doi: 10.1016/bs.abr.2017.11.009

Conflict of Interest: The authors declare that the research was conducted in the absence of any commercial or financial relationships that could be construed as a potential conflict of interest.

Publisher's Note: All claims expressed in this article are solely those of the authors and do not necessarily represent those of their affiliated organizations, or those of the publisher, the editors and the reviewers. Any product that may be evaluated in this article, or claim that may be made by its manufacturer, is not guaranteed or endorsed by the publisher.

Copyright © 2022 Gastineau, Li, Ashworth, Witkowski, Turmel, Górecka, Frankovich, Wachnicka, Lobban, Theriot, Otis, Dąbek, Binczewska and Lemieux. This is an open-access article distributed under the terms of the Creative Commons Attribution License (CC BY). The use, distribution or reproduction in other forums is permitted, provided the original author(s) and the copyright owner(s) are credited and that the original publication in this journal is cited, in accordance with accepted academic practice. No use, distribution or reproduction is permitted which does not comply with these terms.